Journal of Theoretical and Applied Information Technology
20th February 2013. Vol. 48 No.2

ISSN: 1992-8645 www.jatit.org E-ISSN: 1817-3195

ONE TYPE TWO-WHEEL SOLAR ELECTRIC BICYCLE BODY MODELING AND SIMULATION

ZHIKUN WANG

Department of mechanical and electrical engineering, Dezhou University, Dezhou 253023,

Shandong,China

ABSTRACT

In this paper a new rounds of solar electric vehicle design and study were carried out on. Application of CAD technology to establish three-dimension geometric model, using the kinetic analysis on the frame and other parts for numerical simulation and static strength analysis for the vehicle model design, virtual assembly, complete frame dynamics analysis and vibration analysis, with considering other factors, first on the frame structure improvement, second on security of design calculation analysis and comparison, finally get the ideal body design.

Keywords: *Solar Energy Electric Bicycle, Intelligent Equipment, Computer Aided Design*

1. INTRODUCTION

In recent years, countries of the world have done a lot of research on solar electric bicycle, but the progress is not obvious [1]. International and domestic, solar electric bicycle production basically is a blank [2] [3].

China is the country of the world's largest producer and consumer of electric bicycles, According to the statistics of the National Bureau of statistics of the enterprises above Designated Size, At present, China electric bicycle industries are confronted with a huge development potential: the production of electric bicycles in 2007 is 19,500,000, in 2008 is 21,300,000, in 2009 is 21,880,000, in 2010 is 23,690,000, in 2011 is 25,180,000, expected to more than 27,500,000 in 2012 [4] [5].

The foreign car companies are actively studying on the solar car, domestic car companies study less, But because of the cost of solar cars cost hundreds of thousands RMB, which not conducive to large-scale and the low cost of promotion., Solar electric bicycle cost is not so much, about four thousands RMB [1], and can also save the charging fees, the domestic market has not such products, so it is expected in the future become the mainstream of the green traffic tools [5].

2. TWO SOLAR VIRTUAL PROTOTYPE ELECTRIC CAR RESEARCH

With the development of virtual prototype technology continues improving, more and more applications of virtual prototyping technology in vehicles [6].The foreign virtual prototyping technology throughout the entire design cycle of new products, comprehensive design analysis tools based on virtual prototyping technology, greatly shorten the product design cycle, reduce product development costs, and improve design efficiency, and in the design of new products stage of the main pharmacokinetic properties of the products such as: security, power, economy, comfort and structure dynamic characteristics, strength, stiffness, dynamic stress, fatigue life accurate prediction and assessment [7], in a timely manner for defects and deficiencies to be improved ,which optimized to ensure that the product has a good performance and strong market competitiveness. Vehicle simulation electric bicycle application of virtual prototyping technology can be evaluated and optimized electric bicycles, comfort, handling, and use of the finite element method components simulation analysis of the components of the static strength and dynamic performance. Dynamic finite element analysis results combined with the theory of fatigue analysis to predict the fatigue strength of the parts in a variety of conditions using [8], virtual prototyping technology electric cars to achieve a virtual analysis of electric bicycles, instead of the previous completed by the physical prototype to work to achieve the level of progress of the design. In the application of electric bicycles, virtual prototyping technology is used to simulate the vehicle's standard experimental simulation for the various parameters and the physical prototype test data for comparison under the same conditions, thereby providing the

Journal of Theoretical and Applied Information Technology
20th February 2013. Vol. 48 No.2

ISSN: 1992-8645 www.jatit.org E-ISSN: 1817-3195

data, to achieve the precise application of the virtual prototype model [9].

Virtual prototyping technology for electric bicycle parts with this thesis; independent design and utility model intellectual property patent two solar electric cars as a case study, as shown in Fig. 1. The virtual prototype model of solar electric bicycle frame to establish major research determined, load and boundary conditions, the dynamic response of the electric vehicles in use in the simulation, component fatigue life prediction, optimization and improved design. The frame structure of the seat frame, windshield, steering wheel, seat and backrest, battery boxes, brake systems, solar tracker light system. The frame structure sheet metal stamping parts, the parts of the sheet structure to enhance the structural strength and stiffness. The 10th frame material quality carbon structural steel, 40Cr material is part of the shaft and sleeve parts used.

Because most of the actual frame structure is made of thin-walled sheet metal plates and shell trailers finite element model for simulation analysis using shell elements. Geometrically finite element modeling of the frame virtual prototype analysis of the main components of the electric bicycle body, kinetic and static strength analysis of the frame, complete frame transient dynamics analysis and vibration characteristics of the frame analysis.

Figure 1: The Body Designs Of The Solar Electric Vehicle

3. MODEL ANALYSIS OF FRAME STRUCTURE

Establish the geometry entity model frame in the PRO/E environment, using Mechanica module of the finite element analysis model is established. Dynamiting finite element analysis to obtain the entire body structure of the natural frequencies and mode shapes, study the problem from a holistic perspective, some of the details of the structure of the problem can be ignored, and the degree of regularity of the unit is also relatively small impact on the calculation results, as shown in Fig.2.Two models are used in the analysis process, a model cell size is 5mm,the model retained most of the details of the structure, including rounded, attachments, etc., another model unit size of 10 mm, ignored in the model rounded and do not affect the overall characteristics of structural features. Little difference calculation of the two models of the first natural frequency, vibration mode is also very consistent, that affect the results of the model form and parameters of the structure, a model analysis results after the design is taken, this could be assured calculation accuracy, but also to save computer resources. Model extraction using subspace method, this method of high accuracy, strum sequence and the algorithm to calculate whether tainted root monitor, the downside is that the calculation time is relatively slight increase. The model analysis model is shown in Fig.3.

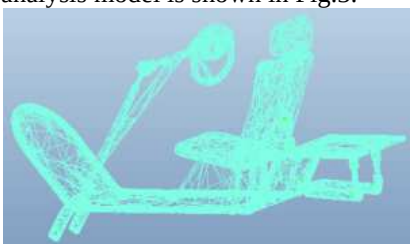

Figure 2: The Frame Finite Element Model

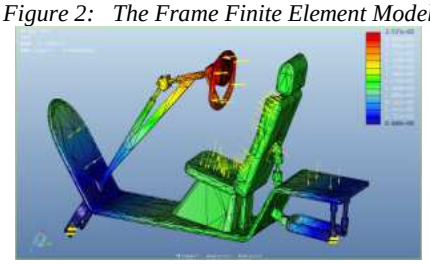

Figure3: The Model Analysis Models

Table 1: Frame Model Results Table

Machine Name	Hz
The First order vibration	***90.433***
The Second order vibration	***96. 90***
The Third order vibration	***135.40***
The Fourth order vibration	***168.70***
The Fifth order vibration	***210.20***
The Sixth order vibration	***250.20***
The Seventh order vibration	***260.30***
The Eighth order vibration	***278.02***
The Ninth order vibration	***361.32***
The Tenth order vibration	***375.48***

The design of the frame were calculated in the free model and the 10 order natural frequency and vibration mode, the model analysis results are shown in Table 1, its characteristics are analyzed as follows:

The First order vibration model: frequency 90.433Hz overall bending mode. Bending vibration section line is located in the frame within the symmetry plane of the two lines. Central one in the head portion of the frame in the end tube and

ISSN: 1992-8645 www.jatit.org E-ISSN: 1817-3195

another semicircular opening in the frame composition of the middle two lines of the rear area of the rear of the seat on the "U" shape, frame within the part of the semicircle, and is located outside the upper half portion in opposite direction of vibration.

The Second order vibration model: frequency 96.905Hz overall bending mode. The bending vibration section line perpendicular to the frame side of the two lines, respectively located in the frame front position and the junction of the seat and the rear luggage rack, from the frame side view you can see the two lines in the middle part other than the part of the two lines was vibrating in the opposite direction, and the farther away from the pitch line is the amplitude of the larger front bezel, steering wheel, seat back the central frame tail modes abdomen area.

Figure 4: The First Order Vibration Model

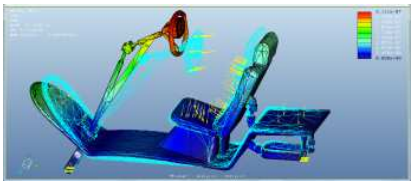

Figure 5: The Second Order Vibration Model

The Third order vibration model: torsion model frequency 135.40Hz overall bend. The frame for space sheet metal structure, the torsion vibration of the section line is located in the middle of the junction of the seat and rear luggage rack along the seat back until the pedal middle curved section line located on the frame and on the beam of between. See from the animation frame vibration, part other than the part of the middle of the pitch line and two lines were vibrating in the opposite direction, the larger the amplitude and farther away from the pitch line, such as the windshield frame, steering wheel and seat back connection to the abdominal area of the part of the frame luggage rack damping spring connection modes.

The Fourth order vibration model: frequency 168.70Hz overall second order bending mode. Its bending vibration of the section line perpendicular to the frame side of the three lines, strengthen tendons and baffle connection at one located on the front, one in the rear luggage rack with the middle of the frame at the connection point rearward, the other one is located in the seat The back-end luggage rack is connected at the upper part. Each pitch line on both sides of the vibration are in opposite directions, the connection of the luggage rack and a seat back at the maximum amplitude, and this place the direction of movement opposite to the direction between the two lines in the whole, this is the structure causes here by the reverse extrusion. The front baffle, spring shock absorber mounted lug the end of the luggage rack shapes the abdominal area.

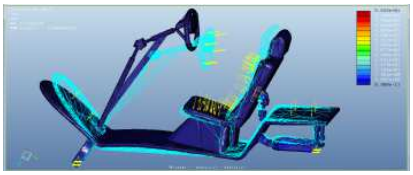

Figure 6: The Third Order Vibration Model

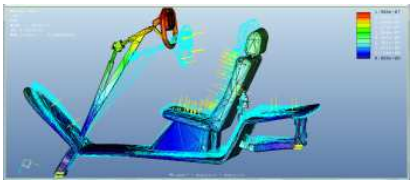

Figure 7: The Fourth Order Vibration Model

The Fifth order vibration model: model frequency torsion modes 210.20Hz overall order. The pitch line is located in the torsion vibration of the two lines in the frame side center plane. A is in the frame header, and the other one is located in the middle of the frame seat downwardly along the junction of the rear tube, with the front body. Opposite the pitch line both sides of the torsion vibration direction, due to the frame for space structure vibration modes from the animation seems more complicated, the end of the luggage rack on both sides of the maximum amplitude, chassis front are relatively small amplitude.

The Sixth order vibration model: frequency of the torsion mode 250.20Hz the frame space sheet metal structure. Baffle central to the pedal lower part of the direction of the location of the first half of the section line, connected to the latter part of the frame seat and luggage rack at the middle to the pedal after pipe connection at the section line. The combination of two parts, vibration in the front and rear parts of the connection, frame the middle part of the amplitude smaller the frame tail on both sides and seat the middle of the vibration abdomen.

Journal of Theoretical and Applied Information Technology
20th February 2013. Vol. 48 No.2

ISSN: 1992-8645 www.jatit.org E-ISSN: 1817-3195

Figure 8: The Fifth Order Vibration Model

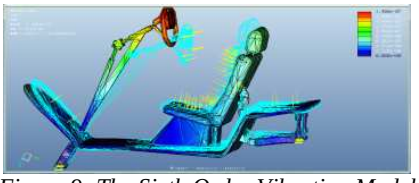

Figure 9: The Sixth Order Vibration Model

The Seventh order vibration model: the frame frequency 260.30Hz overall torsion modes. Baffle central to the pedal lower part of the direction of the location of the first half of the section line, connected to the latter part of the frame seat and luggage rack at the middle to the pedal after pipe connection at the section line. Pitch line on both sides opposite to the vibration direction. The maximum amplitude that the connecting portion of the upper universal joint in the steering wheel, the seat back and at the luggage rack connecting the abdominal region of the vibration.

The Eighth order vibration model: Frequency 278.02Hz the overall third-order bending mode. Frame symmetry plane bending vibration, the vibration of the section line perpendicular to the frame side, one is located in the Central ribs centers, one located in the pedal rear, one is located in the seat back end, and another one in the middle of the lower luggage rack. Section line both sides of the vibration in the opposite direction, the larger the amplitude is farther away from the pitch line. The connection of the front bezel of the middle of the steering wheel in the upper part of the seat and pedal connections, the seat backrest and luggage rack, luggage rack lower junction, etc. to the vibration of the abdomen. The greatest amplitude appears in the upper part of the steering wheel, the minimum front bezel with pedal connected at the position.

Figure 10: The Seventh Order Vibration Model

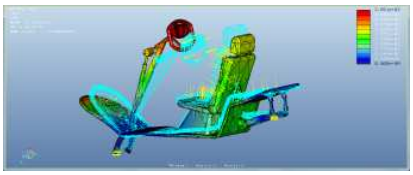

Figure 11: The Eighth Order Vibration Model

The Ninth order vibration model: 361.32Hz overall frequency of third-order bending mode. Frame front bezel of the front of the steering wheel the upper end, the upper part of the seat back and the nursing pillow junction, the forward position of the middle of the luggage rack is the vibration of the section line. Pedal and the seat of the connection at the junction of the upper part of the seat, luggage rack, luggage rack at the connection of the lower end of the base plate in the seat back vibration abdomen. Vibration maximum appear in the upper part of the baffle front end and steering wheel.

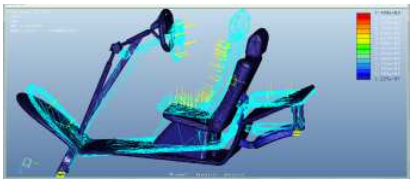

Figure 12: The Ninth Order Vibration Model

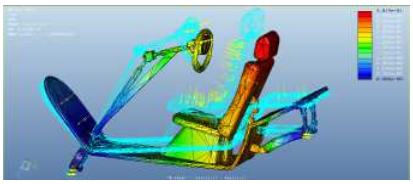

Figure 13: The Tenth Order Vibration Model

The Tenth order vibration model: frequency torsion model 375.48Hz bend. The frame in the rear and tail do bending vibration, the tail portion torsion vibration. The middle bending vibration section line in the middle of the stiffener, and the steering wheel vibration in the same direction. The pitch line of the rear of the bending mode in the frame side, the front end position of the luggage rack. The middle section of the torsion vibration line from the luggage rack and seat back the junction damping spring mounting lug welded at along the pedal down. Steering wheel, the upper end of the pedal back-end, the junction of the seat back with the nursing pillow, seat backrest and luggage rack connections vibration abdomen, vibration in the upper part of the largest in the seat backrest.

4. FRAME STATIC STRENGTH ANALYSIS

Journal of Theoretical and Applied Information Technology
20th February 2013. Vol. 48 No.2

ISSN: 1992-8645 www.jatit.org E-ISSN: 1817-3195

4.1 Frame Structural Features and the Modeling Process

Frame static analysis model shown in Fig. 14. The frame has a symmetrical structure, mainly composed of complex sheet metal structure of the space and the space of plate and shell structures, baffle, pedal, seat, luggage rack space sheet metal structure reinforcing plate before spring shock absorber mounting lug and pedal space Shell structure, seat bottom part of the frame structure for the main bearing components. For Finite Element Analysis, Frame Central and the second half is the focus of the research division of the unit should be as far as possible refinement.

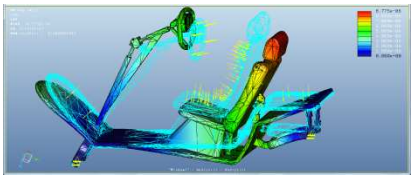

Figure 14: Frame Static Analysis Of Finite Element Model

Its purpose to calculate the frame throughout the stress and deformation, for static's finite element analysis, especially frame carrying the most sensitive areas of stress and deformation. Finite element model is established, should both be considered as a whole, but also consider local.

The first program using the shell element with a thickness of 10mm frame discrimination. The fence head, the baffle and the pedaling connections, since they are not the main bearing member, its structure discrimination can consider rough, in order to save calculation time, while for the left of the seat rails, pedaling, and luggage rack, right connection plate, since they are the most sensitive parts of the frame carrying them when discrimination meticulous, including some of the structural details of the left and right connection plate to be considered, the junction of the seat back with the luggage rack of the luggage rack, to replace the unit with a spring, the law of motion of the suspension through the establishment of the spring unit two nodes constraint equations to describe, frame static's establish finite element model of the 38,319 units, 37,515 nodes and 423,739 degrees of freedom. Practice has proved that, for about 10 minutes to solve the time required for the CPU to 2.60GHZ Intel Pentium i5 Series.

Preliminary calculations, spring shock absorber lower mounting lug frame welding stress about 290MPa. The reason why such a situation is due to the spring shock absorber with the spring means in place, the lower end of the spring means in a fixed constraint, so the analog mode and the physical model are too different, the result of the calculation error is relatively large, and ultimately not adopted.

Second program shell element discrimination thickness of 15mm, According to this idea of establishing the frame static's 19,242 units in the finite element model, 9978 nodes, 65008 DOF. Omitted spring damper at the front bezel to establish the connection quality tube unit, quality management unit two nodes using constraints, and in the spring damper installed lug rear fork plate after connection the board mounting the axial end portion of the external force is applied, the size of these forces is the use of the ADAMS analysis software determined. Table 2 lists the load data for static analysis; static analysis results are given in Table 3. Solving time is about 1 minute on the CPU to 2.60GHZ Intel Pentium i5 Series.

Table 2: Frame Model Results Table

Loading parts	Y direction (N)	Z direction (N)
Rear fork plate	***-850.13***	***6524.70***
After connecting plate	***-10803.43***	***1026.65***
Damper lug	***17639.12***	***-5412.68***

Table3: Static Analysis

Loading cases	Structural position	Stress values (MPa)
Static loading	***Front-end Max***	***42.9***
	Lug Max	***86.8***
	Tail Max	***18.3***
	Pedal Max	***225.09***

4.2 The Frame Static Analysis Results

The second program in the handling closer to a real physical model, using the results of the second program, the stress intensity distribution: the front-end and tail stress cloud display range is from 0 to 55MPa, frame lug stress cloud stress range is from 0 to 95MPa, large parts of pedaling stress cloud display range is from 0 to 195MPa. Frame the front and the entire second half of the stress values were less than 50Mpa, and only a few more than 20MPa. Spring shock absorber mounting lug at the lower part of the frame welding stress close to 100MPa, roots of the frame on the rear fork board, after connecting plate and the overall chassis welding stress exceeds 200MPa. Only one node of the stress is too large for the lower part of the lug of the spring shock absorber and at the frame welding, to 100Mpa, the surrounding nodes stress rapidly reduced to only the 20-30MPa, here there is a significant stress concentration phenomenon, This is because the structure here is the way to connect

Journal of Theoretical and Applied Information Technology
20th February 2013. Vol. 48 No.2

ISSN: 1992-8645 www.jatit.org E-ISSN: 1817-3195

with welding, handling a limited member of the model after this point lug only one unit with four of the luggage rack unit phase, in fact structural change is not so dramatic, and so produce excessive stress adding unit, where the stress value will drop after the model close to the actual situation.

This part of the pedal rearward, first force comparison great two opposite direction size has 9000-12000N force acting on this part, Further the structure of this part of the rear connecting plate is a lever form, and the parts of the force arm length, supporting parts and the overall chassis welding, short arm, the rear fork plate frame roots is also leveraged structure.

4.3 The Frame Static Stress Distribution and Structural Strength Evaluation

View from the frame static stress distribution, the first half of the frame and pedal connected at the stress value is low, appeared to be very surplus material is not fully utilized, and frame the central region, the stress values above 50Mpa close even more than the allowable stress limit, high material utilization, and individual area, after connecting plate and the overall chassis welding and after connecting plate and the overall chassis welding, stress concentration.

From the point of view of the theory of static strength, the frame front and tail force, low stress values, which the Ministry of the force is too large, almost even more than the allowable stress values higher stress. Therefore, only from the standpoint of static stress distribution, the front and rear portions of the frame are relatively safe, in particular the rear wheel suspension member of the partial hazard.

As shown in Fig. 15. this condition pedaling rear end of the luggage rack connected at the upper portion of the large stress here stress occurs in the process of the electric vehicle frame over the crown of the two peaks can be seen from the curve, this is because when the front and rear wheels by uneven road, the electric car as a whole respectively, by two impact load intermediate car body twice the impact on this process, a falling load is relatively small, so the stress is a minimum value. From the analysis results of the special conditions of the frame, the maximum stress value is beyond the scope of allowable stress so when this part of the pedal on the high-speed electric vehicles through the uneven pavement barriers are likely to destroy.

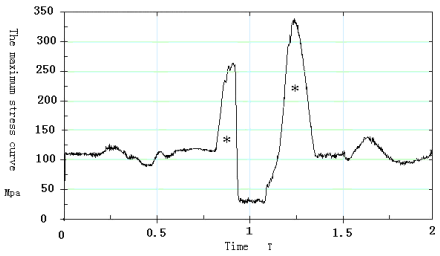

Figure 15: The Pedal Maximum Stress Curve

5. FRAME STRUCTURE IMPROVEMENTS AND IMPROVED RESULTS

From the previous analysis, the strength of the frame is the weak point in the seat-back back-end and spring damper installed lug parts. Parts of structural strength and the deformation force after the pedal has a problem, in the use of the easiest to destroy, mounting lug portion of the spring damper spring connecting member can not meet the requirements of the fatigue strength and the long-term use may produce fatigue breaking.

Analysis results on the structure of the frame a few suggestions for improvement:

1. Add the connection to the top of the spring damper mounting lug on the support member in the seat back, after installation the finite element model shown in the left of Fig. 16.

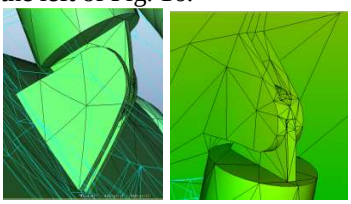

Figure 16: After The Installation Of Finite Element Model

2. Rely behind spring shock absorber mounting lug on beam welding at the seat do rounded, smooth over joints, eliminating stress concentration left of the finite element model is shown in Fig. 15.The modified lug the geometric model is shown in Fig.17.

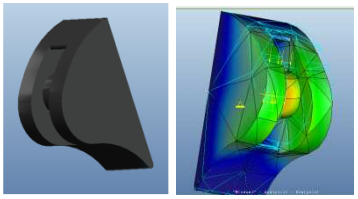

Figure 17: Improved Support Lug

3. Add stress is maximum motherboard ribs increase structural strength, this improved structure shown in the right of Fig. 15.

4.Increase the overall thickness of the motherboard, the motherboard overall thickening to

Journal of Theoretical and Applied Information Technology
20th February 2013. Vol. 48 No.2

ISSN: 1992-8645 www.jatit.org E-ISSN: 1817-3195

5mm. Add some programs stress pedaling on large parts of the ribs, or do the step surface, doing a reasonable distribution of a certain role in reducing the maximum stress and the stress but taking into account technological factors and cost problems eventually gave up these modifications.

Spring damper installed in the same boundary conditions as the original model is applied to the improved model again analyzed and calculated from the results according to the method one.

The modified calculated as shown in Table 4 static analysis, improved static stress distribution is shown in Fig.18. The front bezel and tail stress cloud shows range from 0 to 50Mpa, lug stress cloud the display range is from 0 to 100Mpa pedaling stress relatively large parts of the stress of the stress cloud display range is from 0 to 200Mpa.

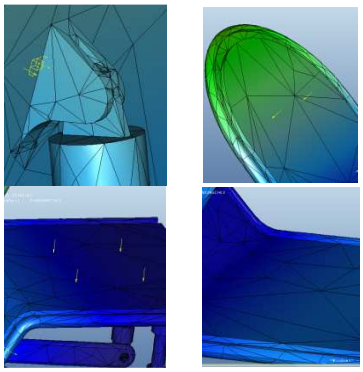

Figure 18: Improved Frame Static Analysis Of The Stress Cloud

Table 4: Static Analysis Of The Resulting Data Table

Working conditions	Structural position	Stress values MPa
Static load	***The front bezel Max***	***42.3***
	Lug Max	***58.4***
	Tail Max	***22.4***
	Pedal Max	***162.3***

As can be seen from the results of the analysis of Table 4: improved after most of the structural stress in the overall frame are less than 100MPa, only the seat back between the mounting part of the damper arm mounting portion on the rear swing arm has a small more than 100MPa, the maximum stress in the case of static 162.3MPa, have relatively large reduction than the improvement to reach the range of the allowable stress requirements.

Transient analysis result of improved look frame, Fig. 19. is a the stress graph showing the transient analysis of the improved frame, the top in the figure is a graph of the spring shock absorber mounting part, the following is the stress curve of the pedal parts. Can be found the site two stresses on the frame in the stress level of the entire work process has significantly decreased, suggesting that the changes made for the conclusions of the previous analysis produces fairly good results. And the entire work process frame stress does not exceed the allowable stress.

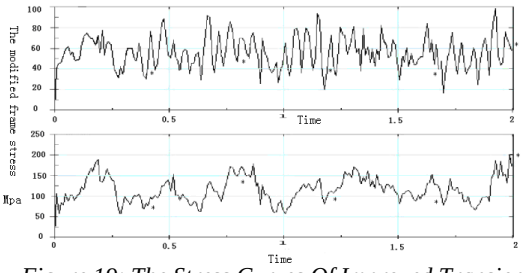

Figure 19: The Stress Curves Of Improved Transient Analysis Frame

Table 5: Improved Frame Stress Rams Before And After Comparison Table

Location	Unimproved Mpa	Improved Mpa
Spring damping lug parts	***139.85***	***92.76***
After fork installed parts	***215.14***	***124.10***

Table 5 is to improve the front and rear frame stress rams comparison table, the table lists several options improved frame spring shock absorber mounting lug and rear fork mounting parts of the stress rims stress misrepresents the statistical value of the average vibration energy of the various parts of the frame in the work process, the rams smaller energy is smaller, the structure in the work process is less easy to destroy. Rams before and after the program improvement has a relatively large decrease in the values in the table also shows the improvement program has played its due role.

6. CONCLUSION

The new two solar electric bicycle bodies to evaluate the static strength and dynamic characteristics of the electric vehicle frame, press modifications proposed several modifications to the operation, through a large number of examples, summed up some electric bicycle frame structure and structural parameters of the frame static strength and dynamic characteristics studied. Also analyzed the vibration performance of electric vehicles, using the finite element model frame structure parameters and structure of the vibration performance, improved frame vibration analysis and in accordance with the electric bicycle, electric bicycles overall improved mechanical properties have been improved.

ISSN: 1992-8645 www.jatit.org E-ISSN: 1817-3195

ACKNOWLEDGEMENTS

This work was supported by Shandong province science and technology projects (2012YD04024), and was supported by DeZhou science and technology projects (2012B07).

REFERENCES:

[1] Zhiqiang Xu, Xingbo Shil, "The Development of Solar Electric Bicycle", *Micro computer information*, Vol. 32, No. 11, 2006, pp. 30-32.
[2] Li Jun, "New solar cell board: a new device of solar electric bicycle", *Chinese invention patent*, Vol. 1, No. 10, 2010, pp. 118.
[3] Zhongchao Ma, "The three meeting of the seven session of the China Bicycle Association", *China bicycle*, Vol. 2, No. 1, 2011, pp. 14.
[4] Liu.X.,LoPes.L.A.C., "An improved Perturbation and observation maximum Power Point tracking algorithmic for PV arrays", *Power Electronics Specialists Conference*, Vol. 5, No. 3, 2010, pp. 66-68.
[5] Brinkworth,B.J.,Marshall,R.H., and Ibrahim,Z., "A Validated Model of Naturally Ventilated PV Cladding", *Solar Energy*, Vol. 69, No. 4, 2000, pp. 67-81.
[6] TriPanagnostoPoulos,Y.,Nousia,T.,Souliotis,M .,andYianoulis,P.,Hybri, "Photovoltaic-Thermal Solar System", *Solar Energy*, Vol. 72, No. 6, 2002, pp. 217-234.
[7] B.Marion, "A method for modelling the current-voltage curve of a PV module for out door condition", *Research and Application*, Vol. 10, No. 3, 2002, pp. 205-214.
[8] William R.Cawthorne,Parviz famouri,Jingdong Chen, "Development of a Linear Alternator-Engine for Hybrid Electric Vehicle Applications", *IEEE Transactions On Vehicular Technology*, Vol. 48, No. 6, 1999, pp. 289-314.
[9] E.Esmailzadeh,G.R.Vossoughi A.Goodarzi, "Dynamic Modelling and Analysis of a Four Motorized Wheels Electric Vehicle", *Vehicle System Dynamics*, Vol. 35, No. 3, 2001, pp. 48-52.
[10] Lino Guzzella ,Alois Amstutz, "CAE Tools for Quasi-Static Modelling and Optimization of Hybrid Power trains", *IEEE Transactions on a Vehicular Technology*, Vol. 48, No. 6, 1999, pp. 158-164.